SCIENCE CHINA
Information Sciences

• **RESEARCH PAPER** •

December 2017, Vol. 60 122501:1–122501:8
doi: 10.1007/s11432-016-0569-2

Quantum correlations generation and distribution in a universal covariant quantum cloning circuit

Xijun REN

School of Physics and Electronics, Henan University, Kaifeng 475000, *China*

Received August 23, 2016; accepted October 30, 2016; published online April 1, 2017

Abstract We discussed the distribution and generation of quantum correlations in a universal covariant quantum cloning circuit. Specifically, we first considered the distribution of quantum correlation, i.e., quantum discord, among the four qubits of the circuit. Then, we analyzed the generation of genuine 3- or 4-qubit entanglement in the cloning process. It is found that the circuit generates genuine 4-qubit GHZ (Greenberger-Horne-Zeilinger)-type state while only W-type 3-qubit state could be generated. These results illustrate the special quantum correlation manipulation capabilities of the cloning circuit.

Keywords quantum information, quantum correlation, quantum discord, universal covariant quantum cloning circuit, genuine multipartite quantum correlation

Citation Ren X J. Quantum correlations generation and distribution in a universal covariant quantum cloning circuit. Sci China Inf Sci, 2017, 60(12): 122501, doi: 10.1007/s11432-016-0569-2

1 Introduction

As is well known, an unknown quantum state cannot be perfectly cloned [1], however, it is possible to design so called quantum cloning machines that can create optimal copies under quantum restrictions [2,3]. Besides the optimal redistribution of quantum state information among all the output copies, quantum cloning machine, as a physical process with nonlocal operations, also introduces changes into the distribution of quantum correlations. As an essential resource for quantum computation and communication, quantum correlations are almost ubiquitous in different quantum information processes [4]. So it would be interesting and important to investigate the evolution of quantum correlations under these processes [5–8].

Here, we will first investigate the distribution of bipartite quantum correlations in a universal covariant quantum cloner (UCQC) designed by Bužek et al. [9, 10] for qubits. UCQC opens the research on both symmetric and antisymmetric quantum cloning. It is important to notice that there are many different quantum correlation measures which are defined towards different information tasks. In [11], Szabó et al. discussed the distribution of concurrence [12], a correlation measure of resource for quantum teleportation, in UCQC. Here, we will consider quantum discord [13], which is a correlation measure of quantum resource for one-way deterministic quantum computation [14, 15]. Compared with concurrence, we find some new features for the distribution of quantum discord.

Email: renxijun@mail.ustc.edu.cn

Besides the bipartite correlation, a multipartite quantum system could also have genuine multipartite correlations that correlate more than two subsystems. Even more interestingly, the subsystems in a multipartite quantum system can be entangled in different ways, e.g., three qubits can be entangled in two inequivalent ways [16] and four qubits in nine different ways [17]. For qubit systems, invariants under stochastic local operations and classical communications (SLOCC) have been introduced to measure genuine multi-qubit correlations [18, 19]. Here, we will consider the generation of genuine multipartite correlations by UCQC. Based on the calculation of SLOCC invariants, we find that, with four qubits input, the generated four qubits entangled state is a GHZ-type state; while with three quibts input, the output state is a three qubit W-type state.

2 Analysis of universal covariant quantum cloner

Before expanding our results, we will first provide an insightful analysis on the UCQC circuit in Figure 1 in [11]. The circuit operates on three qubits denoted as 2, 3, 4. In ports 2 and 3, the original qubit and the first ancilla output the two clones, and the other ancilla in port 4 outputs an anti-clone qubit. Here one qubit of a two-qubit entangled state $|\Phi^{(\text{in})}\rangle$ in port 2 is taken as the input state, therefore, counting in the reference qubit in port 1, we have four qubits altogether. The state input in ports 3 and 4, $|\Psi^{(\text{prog})}\rangle$, is denoted as program state because it determines the transferring of the original state to the two clones. The final output state of the four qubits depends on their initial state, which also determines the distribution of the quantum information and correlations.

The initial state is a direct product of two pure states,

$$|\Phi^{(\text{in})}\rangle_{12}|\Psi^{(\text{prog})}\rangle_{34} = (\sqrt{C}|00\rangle + \sqrt{1-C}|11\rangle)_{12} \otimes \mathcal{N}[\alpha|0\rangle(|0\rangle + |1\rangle) + \beta(|00\rangle + |11\rangle)]_{34}, \tag{1}$$

where, $\alpha + \beta = 1$ and normalization constant, $\mathcal{N} = 1/\sqrt{2(\alpha + \beta^2)}$. After the cloning operations, this state evolves into

$$\begin{aligned}|\Psi^{(\text{out})}\rangle = \mathcal{N}[&(\sqrt{C}|0000\rangle + \sqrt{1-C}|1111\rangle) + \alpha(\sqrt{C}|0101\rangle + \sqrt{1-C}|1010\rangle)\\ &+ \beta(\sqrt{C}|0011\rangle + \sqrt{1-C}|1100\rangle)]_{1234}.\end{aligned} \tag{2}$$

In (2), the expression of the state is carefully organized to show the distribution of original entangled state $|\phi^{(\text{in})}\rangle$ and the asymmetry between the two output copies, qubits 2-3. Exchanging these two copies, we notice that only the places of α, β are changed, which shows the asymmetry of the cloning circuit defined by the programmed state $|\psi^{(\text{prog})}\rangle_{34}$. This insight has clear interpretations in terms of the cloning circuit. Some simple and direct derivations following the cloning circuit operations illustrate that, $|0\rangle_3(|0\rangle + |1\rangle)_4/\sqrt{2}$, $(|00\rangle + |11\rangle)_{34}/\sqrt{2}$, the two superposing pure states in the programmed state have special contributions with respect to the cloning task. When the initial input state is $|0\rangle_3(|0\rangle + |1\rangle)_4/\sqrt{2}$, irrespective of the state at copy 2 is pure or mixed, it will be transferred to copy 3 by the circuit, and meanwhile the qubits 2-4 will result in a maximally entangled state. Of course, this means that the cloning circuit clones the quantum information at qubit 2 completely to qubit 3. It should be pointed out that, not only the local information at qubit 2, but also its quantum correlations, here with the purifying qubit 1, are also cloned to qubit 3. However, with initial state $(|00\rangle + |11\rangle)_{34}/\sqrt{2}$, interestingly, nothing happens to all the four qubits. Therefore, this state is kind of a fixed-point state for the cloning circuit. Certainly, the initial qubit 2 retains all the quantum information and qubit 3 receives no information. When the programmed state, $|\psi^{(\text{prog})}\rangle_{34}$, a superposed state of the above two states, is input to the cloning circuit, asymmetry takes place to the cloning copies 2-3, where the initial quantum information and correlations will be asymmetrically distributed among them. Also we notice that the circuit retains all the original input state information without superposition of other states in the programmed state. Based on this insight of the UCQC circuit, Ren and Fan [20] recently generalized the original circuit to circuit with arbitrary cloning copies and arbitrary dimmentional systems.

In order to calculate the distribution of quantum discords, we will first give some reduced density matrices of the output state where the matrix is represented in the natural basis, $\{|00\rangle, |01\rangle, |10\rangle, |11\rangle\}$,

$$\rho_{12} = \frac{1}{2(\alpha+\beta^2)} \begin{pmatrix} (1+\beta^2)C & 0 & 0 & 2\beta\sqrt{C(1-C)} \\ 0 & \alpha^2 C & 0 & 0 \\ 0 & 0 & \alpha^2(1-C) & 0 \\ 2\beta\sqrt{C(1-C)} & 0 & 0 & (1+\beta^2)(1-C) \end{pmatrix}. \tag{3}$$

As pointed out earlier, ρ_{13} can be obtained from ρ_{12} via exchanging α and β,

$$\rho_{13} = \frac{1}{2(\alpha+\beta^2)} \begin{pmatrix} (1+\alpha^2)C & 0 & 0 & 2\alpha\sqrt{C(1-C)} \\ 0 & \beta^2 C & 0 & 0 \\ 0 & 0 & \beta^2(1-C) & 0 \\ 2\alpha\sqrt{C(1-C)} & 0 & 0 & (1+\alpha^2)(1-C) \end{pmatrix}. \tag{4}$$

Direct calculations from the output state 2 give the reduced state of 1 and 4,

$$\rho_{14} = \frac{1}{2(\alpha+\beta^2)} \begin{pmatrix} C & 0 & 0 & 0 \\ 0 & (\alpha^2+\beta^2)C & 2\alpha\beta\sqrt{C(1-C)} & 0 \\ 0 & 2\alpha\beta\sqrt{C(1-C)} & (\alpha^2+\beta^2)(1-C) & 0 \\ 0 & 0 & 0 & 1-C \end{pmatrix}, \tag{5}$$

with respect to the swaps of two copies 2, 3, i.e., exchanging α and β, ρ_{14} does not change which is reasonable since it should not depend on them. Lastly, we have

$$\rho_{23} = \frac{1}{2(\alpha+\beta^2)} \begin{pmatrix} C & 0 & 0 & 0 \\ 0 & \alpha^2(1-C)+\beta^2 C & \alpha\beta & 0 \\ 0 & \alpha\beta & \alpha^2 C+\beta^2(1-C) & 0 \\ 0 & 0 & 0 & 1-C \end{pmatrix}. \tag{6}$$

3 Distribution of quantum discord

In this section, we will consider the distribution of quantum discord by UCQC. Quantum discord, a measure of quantum correlation, is defined in terms of the difference between quantum mutual information and measurement induced classical correlation in a bipartite system [13]. It quantifies the quantum resource needed for deterministic quantum computation with one quantum bit (DQC1) [14,15]. We first review the definition of quantum discord. For a given quantum state ϱ of a composite system AB, the total amount of correlations, including classical and quantum correlations, is quantified by the quantum mutual information $\mathcal{I}(\varrho) = S(\varrho_A)+S(\varrho_B)-S(\varrho)$, where $S(\varrho) = -\mathrm{Tr}(\rho\log_2\varrho)$ denotes the von Neumann entropy, and ϱ_A, ϱ_B are reduced density matrices for subsystem A, B, respectively. An alternative version of the mutual information can be defined as $\mathcal{J}_A(\varrho) = S(\varrho_B)-\min_{E_k^A}\sum_k p_k S(\varrho_{B|k})$, where the minimum is taken over all possible POVMs (positive-operator valued measures) E_k^A on subsystem A with $p_k = \mathrm{Tr}(E_k^A\varrho)$ and $\varrho_{B|k} = \mathrm{Tr}_A(E_k^A\varrho)/p_k$. Since $\mathcal{J}_A(\varrho)$ quantifies the classical correlation, the difference $D_{A\to B}(\varrho) = \mathcal{I}(\varrho)-\mathcal{J}_A(\varrho)$ defines the quantum discord that quantifies the quantum correlation. The computation of quantum discord for an arbitrary quantum state is notoriously difficult because of the minimization over all possible POVMs or von Neumann measurements in the definition. While much efforts were put, people have calculated quantum discord for only limited classes of states. Among them, two-qubit X

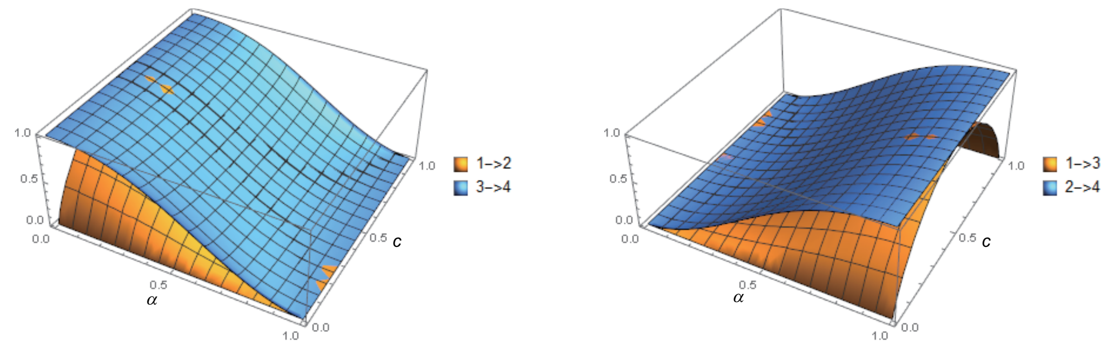

(a) (b)

Figure 1 (Color online) Quantum discords between the following pairs of qubits at the output of the cloning circuits: 1-2, 3-4, 1-3, 2-4. (a) The upper figure corresponds to $D_{3\to 4}$ and the lower one to $D_{1\to 2}$; (b) the upper one corresponds to $D_{2\to 4}$ and the lower one to $D_{1\to 3}$.

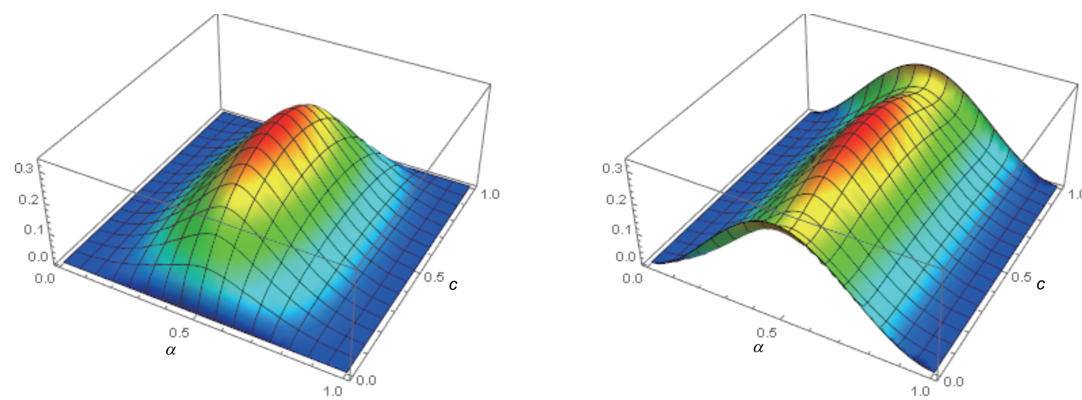

(a) (b)

Figure 2 (Color online) The quantum discord between the following pairs of qubits at the output of the cloning circuit: (a) discord $D_{1\to 4}$; (b) discord $D_{2\to 3}$.

state is an important one [21, 22], whose density matrix takes the form

$$\mathcal{X} = \begin{pmatrix} \varrho_{00} & 0 & 0 & \varrho_{03} \\ 0 & \varrho_{11} & \varrho_{12} & 0 \\ 0 & \varrho_{12}^{*} & \varrho_{33} & 0 \\ \varrho_{03}^{*} & 0 & 0 & \varrho_{33} \end{pmatrix}. \tag{7}$$

In [21], the authors suggested an algorithm to calculate $D_{A\to B}(\mathcal{X})$, which assumes either σ_z^A or σ_x^A be the optimal measurement. Later, some counterexample were found and the precise conditions for optimality with σ_z^A or σ_x^A measurement were found in [22]. These conditions say, the optimal measurement for the quantum discord $D_{A\to B}(\mathcal{X})$ of a real X state $\mathcal{X}$ with $|\varrho_{12}+\varrho_{03}| \geqslant |\varrho_{12}-\varrho_{03}|$ is, (i) σ_z^A if

$$(|\varrho_{12}| + |\varrho_{03}|)^2 \leqslant (\varrho_{00} - \varrho_{11})(\varrho_{33} - \varrho_{22}), \tag{8}$$

and, (ii) σ_x^A if

$$|\sqrt{\varrho_{00}\varrho_{33}} - \sqrt{\varrho_{11}\varrho_{22}}| \leqslant |\varrho_{12}| + |\varrho_{03}|. \tag{9}$$

Considering our reduced two-qubit states of the output cloning state (3, 4, 5, 6), we find that the three reduced states, $\rho_{12}, \rho_{13}, \rho_{14}$ satisfy the condition (8) and σ_z^1 measurement can be used to calculate their discords. Meanwhile, state ρ_{23} satisfies the condition (9) and σ_x^2 measurement should be used to calculate its discord.

Our results are shown in Figures 1 and 2. From Figure 1, one can observe that the discord between qubits 1 and 2 behaves symmetrically in comparison with that between qubits 1 and 3. After cloning operation, for $\alpha = 0$, qubits 1 and 2 are entangled, while for $\alpha = 1$, the discord is transferred to qubits 1 and 3, the clone plays the role of the former original qubit. By continuously tuning cloning parameter α, the discord shared by qubits 1 and 2 could be transferred to qubits 1 and 3. The surfaces representing the discord for the pairs 1-2 and 1-3 are symmetric in the cloning parameter α, that is, they can be obtained from each other by the $\alpha \to 1-\alpha$ substitution, which is also illustrated by the above reduced density matrices. It should be noted that the dependence of these discords from α is monotonous but not continuous: for small values there is a small region where the discord is zero and it appears suddenly and non-continuously. Meanwhile, the dependence of these quantum discords on the initial entanglement in the state, C, is monotonous and continuous.

Another symmetric behavior with respect to $\alpha \leftrightarrow 1-\alpha$ exchange takes place among discords of qubits 2-4 and 3-4. This also could be directly checked by the reduced output state. Here, the $\alpha \leftrightarrow 1-\alpha$ exchange is equivalent to the exchange of qubits 2 and 3. This shows the quantum discord distribution function of the cloning circuit among the clone qubits 2 and 3. In fact, both the discords between qubits 1 and 2, 3, and discords between qubits 4 and 2, 3, are anti-symmetrically distributed by the circuit. We notice that the above features are similar with the results already obtained for concurrence, which illustrates the similarity of the two quantum correlation types under UCQC operation for the above qubit pairs.

However, our calculations show that differences take place for qubit pairs 1-4 and 2-3. In [11], the authors show that qubits 1-4 have zero concurrence and qubits 2-3 have a small amount of concurrence only when the input state $|\Phi^{(\mathrm{in})}\rangle$ is slightly entangled. As illustrated by Figure 2, quantum discord between these qubit pairs behave completely different from concurrence. First, we notice that quantum discord behaves symmetrically with respect to $\alpha \leftrightarrow 1-\alpha$ and $C \leftrightarrow 1-C$ substitutions for both qubit pairs. With a fixed concurrence of the input state, quantum discord increases to its maximum at $\alpha = 0.5$, which takes a maximal value up to 0.33. Second, there are differences between qubits 1-4 and 2-3. For a fixed α, quantum discord between qubits 1-4 increases from zero to its maximum at $C = 0.5$ while the discord between qubits 2-3 changes slightly over the whole area $0 \leqslant C \leqslant 1$. Besides, the comparison between $D_{2\to3}$ and $D_{1\to4}$ shows that $D_{2\to3}$ is always larger than $D_{1\to4}$ and the excess part seems to have origin from the concurrence between qubits 2-3. These results show that, although the UCQC circuit generates no concurrence or entanglement of formation among qubits 1-4 and 2-3, it generates other types of quantum correlation among them. Our results also imply that quantum discord is easier to be generated than concurrence. The above differences between the two types of quantum correlation should come from their definitions. Concurrence of a general density matrix is mathematically defined in terms of all the separable decompositions which may not be physically realizable. However, the decomposition in quantum discord is defined based on measurement which makes it physically accessible. Our results also identify the differences between different types of quantum correlations for mixed states which supplements the previous researches for pure superposed states [23–26].

4 Generation of genuine multi-partite entanglement

Since the UCQC circuit comprises four nonlocal operations among different qubits, along with the copying of the input state, it also produces nonseparable multi-partite quantum state which contains genuine multi-partite quantum correlations. In this section, we will analyze the genuine 4-partite entanglement and 3-partite entanglement in the output state of the cloning circuit with the specified programmed states.

4.1 Generation of genuine 4-qubit entanglement

Four qubits may be entangled in nine different ways. The genuine 4-qubit entanglement in a pure entangled state can be quantified by invariants of stochastic local operations and classical communications (SLOCC). Here we will use the SLOCC invariants measures introduced in [18, 19], the same notations will also be used here. First, we list all the SLOCC invariants with different degrees as follows:

$$H = \sqrt{C(1-C)}, \tag{10}$$
$$L = \mathcal{N}^4 C(1-C)\alpha^2(1-\beta^2), \tag{11}$$
$$M = \mathcal{N}^4 C(1-C)(1-\alpha^2)(-\beta^2), \tag{12}$$
$$N = \mathcal{N}^4 C(1-C)(\beta^2-\alpha^2), \tag{13}$$
$$D_{xy} = \mathcal{N}^6 H^3 \beta^2(1+\beta^2-\alpha^2), \tag{14}$$
$$D_{xz} = \mathcal{N}^6 H^3 \alpha^2(1-\beta^2+\alpha^2), \tag{15}$$
$$D_{xt} = \mathcal{N}^6 H^3 \alpha^2\beta^2(\alpha^2+\beta^2-1), \tag{16}$$

all the SLOCC invariants of a 4-qubit pure state can be obtained from these quantities. Since factor $C(1-C)$ appears in all the invariants, it is obvious that an entangled input state is necessary to produce a genuine 4-qubit entangled state. This is reasonable because the cloning circuit contains no nonlocal operations between the first qubit and the other three. Here, we will calculate the following permutation-invariant measures introduced in [19],

$$|\mathcal{F}_1| = 8[4(D_{xz}+D_{xt}+D_{xy}) - H^3], \tag{17}$$
$$|\mathcal{F}_2| = 16[3H^4 - 16H(D_{xz}+D_{xt}+D_{xy}) - 16(MN+NL+ML)]/3, \tag{18}$$
$$\begin{aligned}|\mathcal{F}_3| = {} & 32\{H^6 + 16H^2[-(M^2+N^2+L^2)+(MN+NL+ML)] \\ & +64(N-M)(L-N)(M-L)\}.\end{aligned} \tag{19}$$

It turns out that, for the cloning output state, we have

$$|\mathcal{F}_1| = \frac{24\beta^2(1-\beta)^2}{(1-\beta+\beta^2)^3}(C(1-C))^{\frac{3}{2}}, \tag{20}$$
$$|\mathcal{F}_2| = \frac{2\beta^2(1-\beta)^2}{(1-\beta+\beta^2)^3}(C(1-C))^{2}, \tag{21}$$
$$|\mathcal{F}_3| = \frac{32\times 27\beta^4(1-\beta)^4}{(1-\beta+\beta^2)^6}(C(1-C))^{3}. \tag{22}$$

Since these monotones have the same dependence on the parameters β, C, they will simultaneously take nonzero values. Therefore, from the SLOCC invariants table for different entangled states constructed in [19], we can determine that the generated genuine multi-partite entangled state belongs to the GHZ-type.

When $\beta = 1$, the cloning circuit will have no effect on the input state and the output state will be a separable state. However, when $\beta = 0$ or $\alpha = 1$, the circuit will generate the most multi-qubit quantum correlations. This also means that the circuit will generate most genuine 4-qubit entanglement when it transfers the original input state to another qubit. In other words, the distribution of qubit information is accompanied with the generation of multi-qubit quantum correlation. The dependence on the initial bipartite concurrence C is explained as follows. When C is very small, i.e., near to zero, since the circuit has no operations to correlate the reference qubit with the others, the generated multipartite correlation is also very small. With the increase of C, the bipartite correlation in $|\phi^{\rm in}\rangle$ contributes to generate multipartite correlation which peaks at $C = \frac{1}{2}$.

4.2 Generation of 3-qubit entangled state

In this scenario, we drop the reference qubit and input the cloner with a single qubit pure state, $|\phi^{\rm in}\rangle = \sqrt{C}|0\rangle + \sqrt{1-C}|1\rangle$. The output state appears to be

$$\begin{aligned}|\Psi^{(\rm out)}\rangle = {} & \sqrt{C}|000\rangle + \alpha\sqrt{1-C}|010\rangle + \alpha\sqrt{C}|101\rangle \\ & +\beta\sqrt{C}|011\rangle + \beta\sqrt{1-C}|100\rangle + \sqrt{1-C}|111\rangle.\end{aligned} \tag{23}$$

Generally, this state is not a separable state since it cannot be written as a direct product state of two subsystems. Three qubits can be entangled in two inequivalent ways, W-type and GHZ-type, which could be distinguished by a correlation measure, three-tangle τ_3 [16]. Specifically, GHZ-type states have nonzero three-tangle while W-type zero. For an arbitrary three qubit pure state, $|\psi\rangle = \sum_{ijk} a_{ijk}|ijk\rangle$, its three-tangle is defined as

$$\tau_3(\psi) = 2\left|\sum a_{ijk}a_{i'j'm}a_{npk'}a_{n'p'm'} \times \epsilon_{ii'}\epsilon_{jj'}\epsilon_{kk'}\epsilon_{mm'}\epsilon_{nn'}\epsilon_{pp'}\right|. \tag{24}$$

Amazingly, when inputting all the coefficients in (23) into this expression, we get $\tau_3(\Psi^{(\text{out})}) = 0$, which means the output state of the UCQC circuit is a 3-qubit W-state.

It should be pointed out that the above analysis are on the output state (23) which comes out of the UCQC circuit with special programmed state $|\Psi^{(\text{prog})}\rangle$. If some other state were input, the output state could have different genuine multi-qubit entanglement. However, since $|\Psi^{(\text{prog})}\rangle$ is specially chosen for the cloning circuit, it is physically interesting to consider them here.

5 Conclusion

Quantum correlations are important resources in quantum information processing tasks, so it is necessary to investigate their distribution and generation in different quantum processes. Quantum cloning machines are a special quantum information process which shows deep difference between quantum theory and classical theory. Here, we provide a detailed investigation on the special capability of this process on the generation and distribution of different types of quantum correlations. We find some new features on the distribution of quantum discord which is different from the distribution of concurrence. This also shows the difference between these two types of quantum correlation. Surprisingly, UCQC also has its special capability on generating genuine 4-qubit GHZ state and genuine 3-qubit W state.

For the future, we notice that our investigations may be further generalized to n-qubit UCQC circuits which was introduced in [20] where qudit case was also introduced. However, the consideration of genuine multi-partite states still poses difficulty since it is difficult to calculate their SLOCC invariants. Besides, it should also be interesting to investigate the manipulation of quantum correlations in other information processing tasks [6–8].

Acknowledgements This work was supported by National Natural Science Foundation of China (Grant No. U1204114).

References

1 Wootters W K, Zurek W H. A single quantum cannot be cloned. Nature (London), 1982, 299: 802–803
2 Scarani V, Iblisdir S, Gisin N, et al. Quantum cloning. Rev Mod Phys, 2005, 77: 1225–1256
3 Fan H, Wang Y N, Jing L, et al. Quantum cloning machines and the applications. Phys Rep, 2014, 544: 241–322
4 Horodecki R, Horodecki P, Horodecki M, et al. Quantum entanglement. Rev Mod Phys, 2009, 81: 865–942
5 Bužek V, Hillery M, Ziman M, et al. Programmable quantum processors. Quantum Inf Process, 2006, 5: 313–420
6 Li J, Chen X B, Sun X M, et al. Quantum network coding for multi-unicast problem based on 2D and 3D cluster states. Sci China Inf Sci, 2016, 59: 042301
7 Zhang Z, Li J X, Liu L. Distributed state estimation and data fusion in wireless sensor networks using multi-level quantized innovation. Sci China Inf Sci, 2016, 59: 022316
8 Wang F, Luo M X, Li H R, et al. Improved quantum ripple-carry addition circuit. Sci China Inf Sci, 2016, 59: 042406
9 Bužek V, Hillery M. Quantum copying: beyond the no-cloning theorem. Phys Rev A, 1996, 54: 1844–1852
10 Bužek V, Braunstein S L, Hillery M, et al. Quantum copying: a network. Phys Rev A, 1997, 56: 3446–3452
11 Szabó L, Koniorczyk M, Adam P, et al. Optimal universal asymmetric covariant quantum cloning circuits for qubit entanglement manipulation. Phys Rev A, 2010, 81: 032323
12 Wootters W K. Entanglement of formation of an arbitrary state of two qubits. Phys Rev Lett, 1998, 80: 2245–2248
13 Ollivier H, Zurek W H. Quantum discord: a measure of the quantumness of correlations. Phys Rev Lett, 2002, 88: 017901
14 Knill E, Laflamme R. Power of one bit of quantum information. Phys Rev Lett, 1998, 81: 5672–5675
15 Datta A, Shaji A, Caves C M. Quantum discord and the power of one qubit. Phys Rev Lett, 2008, 100: 050502
16 Coffman V, Kundu J, Wootters W K. Distributed entanglement. Phys Rev A, 2000, 61: 052306

17 Verstraete F, dehaene J, De Moor B, et al. Four qubits can be entangled in nine different ways. Phys Rev A, 2002, 65: 052112

18 Osterloh A, Siewert J. Constructing N-qubit entanglement monotones from antilinear operators. Phys Rev A, 2005, 72: 012337

19 Ren X J, Jiang W, Zhou X, et al. Permutation-invariant monotones for multipartite entanglement characterization. Phys Rev A, 2008, 78: 012343

20 Ren X J, Fan H. Quantum circuits for asymmetric $1 \rightarrow n$ quantum cloning. Quantum Inf Comput, 2015, 15: 914–922

21 Ali M, Rau A R P, Alber G. Quantum discord for two-qubit X states. Phys Rev A, 2010, 81: 042105

22 Chen Q, Zhang C, Yu S, et al. Quantum discord of two-qubit X states. Phys Rev A, 2011, 84: 042313

23 Ou Y C, Fan H. Bounds on negativity of superpositions. Phys Rev A, 2007, 76: 022320

24 Yu C S, Yi X X, Song H S. Concurrence of superpositions. Phys Rev A, 2007, 75: 022332

25 Song W, Liu N L, Chen Z B. Bounds on the multipartite entanglement of superpositions. Phys Rev A, 2007, 76: 054303

26 Parashar P, Rana S. Entanglement and discord of the superposition of Greenberger-Horne-Zeilinger states. Phys Rev A, 2011, 83: 032301